Anionic Polymerization Mechanism of Acrylonitrile Trimer Anions: Key Branching Point between Cyclization and Chain Propagation

Keijiro Ohshimo,*[1] Yoshiya Inokuchi,[2] Takayuki Ebata,[2] and Koichi Ohno[3]

[1] Chemical Dynamics Laboratory, RIKEN Advanced Science Institute, Wako, Saitama 351-0198, Japan

[2] Department of Chemistry, Graduate School of Science, Hiroshima University, Higashi-Hiroshima, Hiroshima 739-8526, Japan

[3] Toyota Physical and Chemical Research Institute, Nagakute, Aichi 480-1192, Japan

* **Corresponding Author**

E-mail: ohshimo@riken.jp

Current Address of Keijiro Ohshimo

Atomic, Molecular and Optical Physics Laboratory, RIKEN Advanced Science Institute, Wako, Saitama 351-0198, Japan

ABSTRACT: A cluster anion of vinyl compounds in the gaseous phase has served as one of the simplest microscopic models of the initial stages of anionic polymerization. Herein, we describe our investigations into the initial stage mechanisms of anionic polymerization of acrylonitrile (AN; $CH_2=CHCN$) trimer anions. While the cyclic oligomer is found in mass and photoelectron spectroscopic studies of $(AN)_3^-$, only the chain oligomer is found in the infrared photodissociation (IRPD) spectrum of Ar-tagged $(AN)_3^-$. Based on the calculated polymerization pathway of $(AN)_3^-$, we consider that the chain oligomers are the reaction intermediates in the cyclization of $(AN)_3^-$. The rotational isomerization of the $(AN)_3^-$ chain oligomer is found to be the bottleneck in the cyclization of $(AN)_3^-$. To form the $(AN)_4^-$ chain oligomer by chain propagation, the addition of an AN molecule to $(AN)_3^-$ should occur prior to the rotational isomerization. We conclude that the rotational isomerization in the $(AN)_3^-$ chain oligomer is the key branching point between cyclization (termination) or chain propagation in the anionic polymerization.

KEYWORDS: Intracluster reaction, cluster anions, infrared spectroscopy, reaction pathway

1. INTRODUCTION

Strong bases have been shown to initiate anionic polymerization of vinyl compounds that possess electron-withdrawing substituents. In such cases, electron transfer from the strong base causes cleavage of the C=C double bond of the vinyl monomer to yield a carbanion, which then reacts with another monomer to produce a carbanion with a longer linear chain as the propagating species. In some cases, however, undesired cyclization reactions would prevent the propagation of long linear chains. For example, in the anionic polymerization of methacrylonitrile, the polymerization process can be terminated by cyclization of the intermediate trimeric carbanion - the major product was identified as 1,3,5-tricyano-2,4,6-trimethylcyclohexane (cyclic oligomer).[1] Unfortunately, for such polymerizations, the key branching point between chain propagation and cyclization has yet to be elucidated in terms of their elementary reaction processes. Gas-phase spectroscopic studies can offer insight into such elementary reaction processes because the series of oligomers (dimer, trimer, tetramer, and so on) that are produced at the initial stages of the polymerization can be isolated and characterized.[2]

The study of anionic polymerization in the gaseous phase has recently gained much attention.[3-15] A cluster anion of vinyl compounds is one of the simplest microscopic models of the initial stages of anionic polymerization, and accordingly, the studies of acrylonitrile (AN; $CH_2=CHCN$) cluster anions, $(AN)_n^-$, by mass spectrometry, collision-induced dissociation, (near-infrared and visible) photodissociation, and photoelectron spectroscopy have been reported.[7-10,12,15] For mass spectroscopy, magic numbers (intensity anomalies) have been observed at $n=3$, 6, and 9 in the mass spectrum of

the H_2-eliminated AN cluster anions, $[(AN)_n-H_2]^-$ series, which are produced by the electron transfer from a high-Rydberg rare gas atom.[7] These studies gave a conclusion that cyclic trimeric oligomer (1,3,5-cyclohexanetricarbonitrile) is formed by intracluster polymerization (cyclization) of $(AN)_3^-$.

In the present study, we investigated the intracluster polymerization mechanism of $(AN)_3^-$ by infrared photodissociation (IRPD) spectroscopy employing the Ar-tagging method. We also calculated intracluster polymerization pathways including the equilibrium and transition structures by using the GRRM program based on the scaled hypersphere search (SHS) method[16-19,23]. Our IRPD spectrum of $(AN)_3^-Ar$ allowed observations of the trimeric chain oligomers for the first time. Calculations of the polymerization pathway of the $(AN)_3^-$ ions revealed that a trimeric chain oligomer serves as the key reaction intermediate during cyclization, in which its rotational isomerization is a key step whether cyclization or chain propagation occurs in the anionic polymerization.

2. EXPERIMENTAL AND COMPUTATIONAL METHODS

Details of the IRPD experimental setup at Hiroshima University have been described in our previous paper.[20] Although we have attempted to directly observed the IRPD of the $(AN)_3^-$ ions, the ion intensities of the daughter ions were too weak to provide a IRPD spectrum, and therefore, the Ar-tagging method[21,22] of the $(AN)_3^-$ ions was employed. For the IRPD spectroscopy of $(AN)_3^-Ar$ ions, a gaseous mixture of AN (0.005 %) and Ar was expanded into a vacuum chamber through a pulsed nozzle with a stagnation pressure of 0.30 MPa. The pulsed free jet crossed an electron beam at the exit of the nozzle with an

electron kinetic energy of 350 eV.   Cluster ions were accelerated into a flight tube using a pulsed electric field of 1.3 keV.   In the flight tube, the target parent ions, $(AN)_3^-Ar$, were selected by a mass-gate and they crossed an output of a pulsed tunable IR laser.   Daughter ions, $(AN)_3^-$, generated by IRPD were mass analyzed using a reflectron mass spectrometer with a microchannel plate (MCP).   The output signal from the MCP was amplified and fed into a digital storage oscilloscope.   Yields of daughter ions were normalized against the intensity of parent ions and the IR laser.   The IRPD spectra of parent ions were obtained by plotting the normalized yields of the fragment ions as a function of the wavenumbers of the IR laser.   Tunable IR light was obtained using the difference frequency generation (DFG) between the signal and the idler output of an OPO (LaserVision).   The OPO laser was pumped by the fundamental output of a Nd:YAG laser (Spectra-Physics, GCR-250). An $AgGaSe_2$ crystal was used for DFG, and only the DFG output was introduced into the vacuum chamber after the signal and idler outputs were removed using a ZnSe filter.   The power of the IR laser was measured using a laser detector (Ophir, 12A−P).   The output energy was 0.2–1 mJ/pulse in the 1200–2300 cm^{-1} region and 0.1−5 mJ/pulse in the 2000–3200 cm^{-1} region.

To calculate the reaction pathway of the intracluster polymerization of $(AN)_3^-$, the sphere contracting walk (SCW) option[19] in the GRRM program[16-18] was employed the multistep-reaction pathways.   The scaled hypersphere search (SHS) method included in the GRRM program is an uphill walking technique on the potential energy surface starting from a minimum toward saddle points to follow anharmonic downward distortions.   With a downhill-walk algorithm, such as a conventional steepest descent path following

technique, the SHS method is powerful tool for mapping out the global topography of the potential energy surface.[16-18]   Furthermore, the option of 2PSHS in the GRRM program is powerful for finding a saddle point between a selected set of reactant and product.[23]   From the calculated saddle point, the intrinsic reaction coordinate (IRC) calculations can be initiated to confirm the connection between the reactant and the product.   First, the SCW, 2PSHS, and IRC calculations were carried out at the M06-2X/6-31++G** level.   The resulting equilibrium (EQ) and transition state (TS) structures were re-optimized at the M06-2X/aug-cc-pVDZ level.   Zero-point vibrational energies of the EQ and TS structures were corrected at the same level. Energy, gradient, and Hessian were calculated using the Gaussian 09 program package[24].

3. RESULTS AND DISCUSSION

In the mass spectrum, a series of $(AN)_n^-$ cluster ions were observed with $n = 2$–20. The $[(AN)_n-H_2]^-$ cluster ions that were formed by the elimination of a H_2 molecule from $(AN)_n^-$ are also observed.   The size distributions of the integrated ion intensity for the cluster ions are shown in Figure 1.   The magic numbers were observed at $n = 3, 6$, and 9 for the $[(AN)_n-H_2]^-$ series, whereas magic numbers were not observed for $(AN)_n^-$.   This trend is consistent with the mass spectrum of $(AN)_n^-$ cluster ions that were produced by the electron transfer from a high-Rydberg rare gas atom.[7]   The magic numbers can be attributed to the formation of stable cyclic oligomers during the intracluster polymerization of $(AN)_3^-$. The cyclic oligomer anion releases its excess energy that is associated with the cyclization by the elimination of a H_2 molecule.[7]   The occurrence of the same magic

numbers at $n=3$, 6, and 9 for $[(AN)_n-H_2]^-$ in the present setup indicates that $(AN)_3^-$ cyclic oligomers were formed in our cluster ion source.
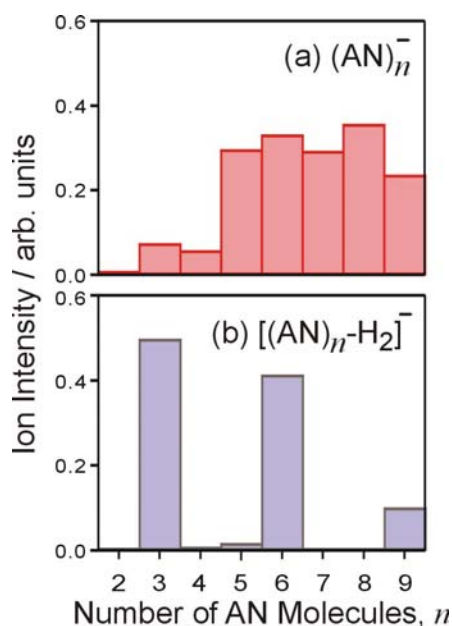
Figure 1. Size distributions of integrated ion intensities in the mass spectrum of (a) $(AN)_n^-$ and (b) $[(AN)_n-H_2]^-$. The ion intensities are plotted as a function of the number of AN molecules (n).

In the case of IRPD spectroscopy of the bare oligomers of the $(AN)_3^-$ ions, photodissociation hardly occurs with a one-photon process because molecules in oligomers are connected by stable covalent bonds. The IRPD of Ar-tagged ions, on the other hand, was effective due to the small binding energy between the ion and the Ar atom resulting in the elimination of the Ar atom from the ion. We believe that structural deformation of the ions due to Ar-tagging is negligible, and thus the observed IRPD spectrum of $(AN)_3^-Ar$ is essentially the same as that of $(AN)_3^-$. As shown in the IRPD spectrum of $(AN)_3^-Ar$ in the 1200–3200 cm^{-1} region (Figure 2a), a strong band is observed at 2080 cm^{-1}, along with several weak bands at 2900-3100 cm^{-1}. Based on previous IR studies on the gaseous

neutral AN molecule,[25] the observed bands in Figure 2a can be assigned as follows: the weak bands at 2900-3100 cm^{-1} correspond to CH stretching vibrations (3034-3133 cm^{-1} in neutral AN), whereas the strong band at 2080 cm^{-1} can be assigned to CN stretching vibration (2240 cm^{-1} in neutral AN).   The red shift of the CN stretching band of (AN)$_3^-$Ar (relative to that of neutral AN molecule) is attributable to the antibonding nature of the CN bond in the (AN)$_3^-$ chain oligomer (see Supporting Information).
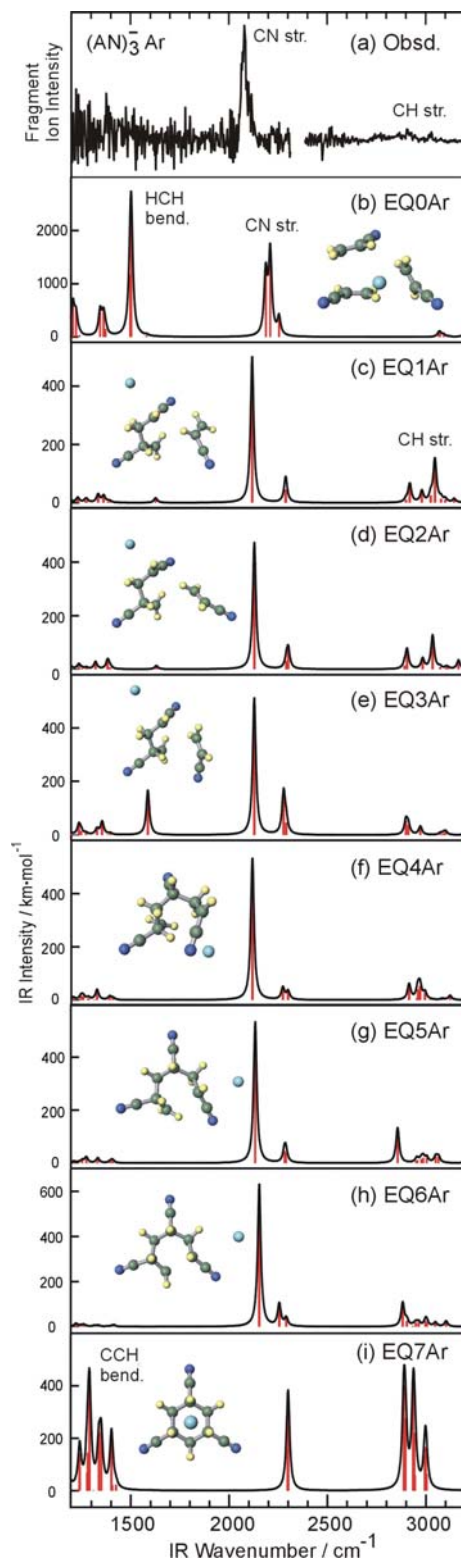
Figure 2. (a) IRPD spectrum of the $(AN)_3^-Ar$ ions. (b-i) IR spectra for isomers EQ0Ar-EQ7Ar calculated at the M06-2X/aug-cc-pVDZ level. Black solid curves were generated by applying the Lorentzian component with full width at a half maximum of 20 cm^{-1} to each IR vibrational band (red bars). Optimized structures of the isomers are displayed in the inserts. To compare the calculated and experimental spectra, the calculated vibrational energies were scaled using a scaling factor of 0.964. The scaling factor was determined from the average ratio between the experimental[25] and calculated frequencies for the normal modes for neutral AN.

To assign the observed bands of the IRPD spectrum, structural isomers of $(AN)_3^-$ was systematically searched by calculations of the polymerization pathway of $(AN)_3^-$ using the SCW method.[19] The energy diagram of the polymerization pathway of $(AN)_3^-$ leading to the cyclic oligomer is shown in Figure 3. For these calculations, the polymerization pathways from the chain oligomer (EQ1) and the cyclic oligomer (EQ7) were investigated. The energy levels of the optimized neutral $(AN)_3$ cluster (EQN), along with the unreacted $(AN)_3^-$ cluster (EQ0) are also shown in Figure 3. The EQN cluster possesses a cyclic structure, involving three NH hydrogen bonds between the three AN molecules. During the electron attachment to EQN, the molecular structures of $(AN)_3^-$ cluster ions started to deform into the stable structure in the anions. Due to the lack of covalent bonds between the three AN molecules, EQ0 was designated as the stable isomer of the $(AN)_3^-$ cluster ions, i.e. EQ0 represents an unreacted cluster. During the initial intracluster polymerization, a CC bond forms between two AN molecules of EQ0, and subsequently, in the EQ1, two AN

molecules become connected through a CC bond, i.e., EQ1 is the AN-solvated $(AN)_2^-$ ion because the electron affinity of $(AN)_2$ is larger than that of the AN molecule.[7]   Despite the presence of a CC bond in EQ1, the energies of EQ0 and EQ1 are comparable presumable due to the stabilization arising from the delocalization of the excess electron in EQ0.   The spatial distributions of the excess electron of these isomers (the singly occupied molecular orbitals (SOMO)) are given in the Supporting Information.   Delocalization of the excess electron over three AN molecules in EQ0 is shown in Figure S1a, whereas localization of the excess electron over a dimeric AN oligomer in EQ1 is shown in Figure S1b.   Our studies have indicated that the stabilization due to delocalization of the excess electron of EQ0 is larger than that of EQ1.   The subsequent formation of EQ2 and EQ3 from EQ1 involves the change in the AN molecule's orientation relative to $(AN)_2^-$.   EQ3 is formed via a 2-step reaction from EQ1 that involves low reaction barriers TS1/2 and TS2/3.   Next, EQ3 undergoes an intracluster polymerization between $(AN)_2^-$ and a third AN molecule via TS3/4 to afford EQ4, which is stabilized by two CC bonds, and is thus more stable than EQ3 by 80.0 kJ/mol.   In the cases of EQ4, EQ5, and EQ6, the AN molecules are connected by covalent bonds.   The EQ4, EQ5, and EQ6 are rotational isomers.   The structures for EQ1-6 can be classified as chain oligomers.   In the final step, EQ6 undergoes intracluster polymerization (cyclization) to afford EQ7, which is a cyclic oligomer (1,3,5-cyclohexanetricarbonitrile) anion, in which all three CN substituents have equatorial conformation.   EQ7 is more stable than EQ6 by 102.0 kJ/mol due to the formation of an additional CC bond.

Among the various steps in the above reaction pathway of intracluster

polymerization of $(AN)_3{}^-$, the reaction barriers of the TS were less than 10 kJ/mol, with the sole exception of TS4/5 between EQ4 and EQ5 (17.5 kJ/mol from EQ4) (Table 1). Investigations were undertaken to gain insight into the reaction mechanism of EQ4 → EQ5. As illustrated using Newman projections (Figure 3), EQ4 and EQ5 are rotational isomers that involve a transition structure possessing an eclipsed conformation (TS4/5). The relatively high barrier energy of TS4/5 is attributable to the steric hindrance between the bulky R_1 and R_2 substituents [$R_1 = -CH(CN)-CH_2$, $R_2 = -CH_2-CH(CN)$].

Table 1. Binding Energies between $(AN)_3{}^-$ Ions and an Ar Atom in $(AN)_3{}^-$Ar Isomers (EQnAr, n=0-7), and Barrier Energies of TSn/(n+1) between EQn and EQ(n+1) Calculated at the M06-2X/aug-cc-pVDZ Level

Isomer Number (n)	Binding Energy in EQnAr (kJ/mol)	Barrier Height of TSn/(n+1) (kJ/mol)
0	7.7	-
1	6.3	8.6
2	4.4	2.4
3	6.3	2.8
4	7.0	17.5
5	5.9	1.3
6	6.5	9.8
7	1.2	-

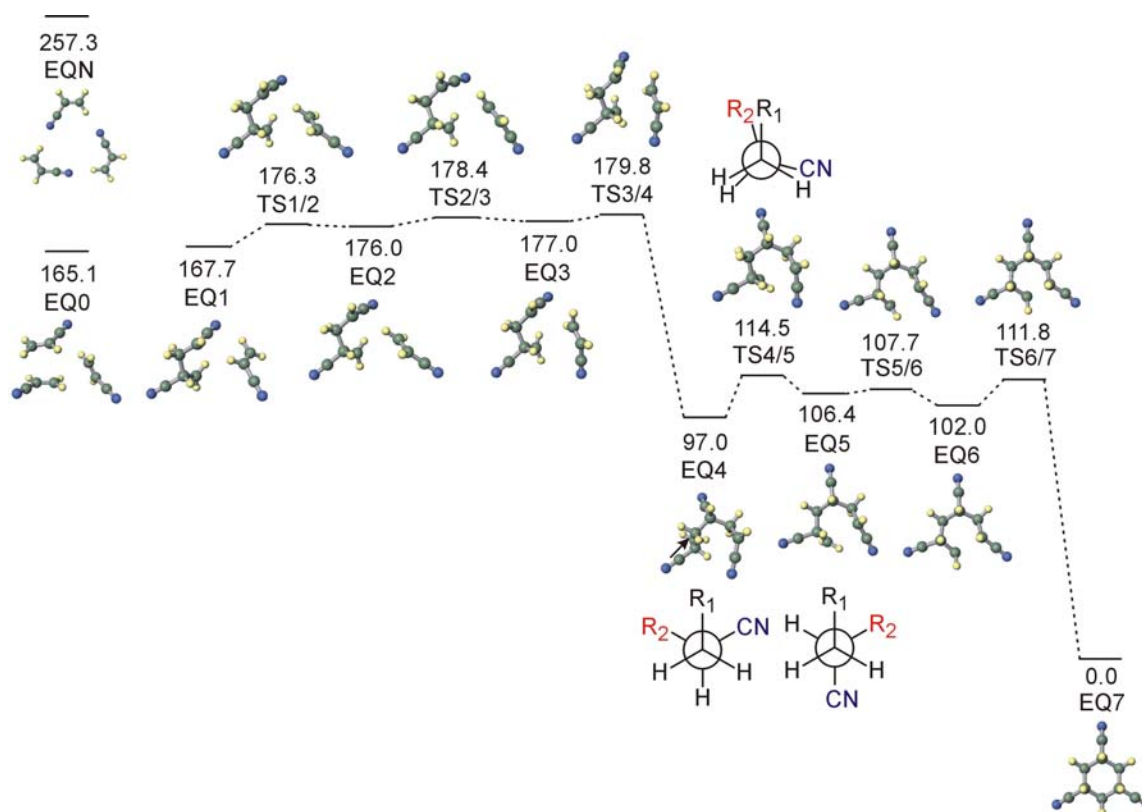**Figure 3.** Energy diagram illustrating the intracluster polymerization pathway of $(AN)_3^-$. The pathway was calculated using the SCW method at the M06-2X/6-31++G** level. Relative energies (in kJ/mol, including zero-point energy corrections) were calculated at the M06-2X/aug-cc-pVDZ level. Newman projections are shown for EQ4, TS4/5, and EQ5; $R_1 = -CH(CN)-CH_2$, $R_2 = -CH_2-CH(CN)$. The Newman projection of EQ4 was derived from the direction as indicated by the arrow.

The vibrational analysis of the $(AN)_3^-$Ar isomers was carried out to assign the IRPD spectrum of the $(AN)_3^-$Ar ions. The IR spectra and optimized structures of the

Ar-tagged EQs calculated at the M06-2X/aug-cc-pVDZ level are shown in Figures 2b-i. Comparisons between the observed and calculated IRPD spectra involved a scaling factor of 0.964, which was obtained from the average ratio between experimental[25] and calculated frequencies of the normal modes in a neutral AN molecule. The viability of the Ar-tagged IRPD spectroscopy was confirmed based on the calculated binding energies between the $(AN)_3^-$ (EQ0-7) ion and an Ar atom – as listed in Table 1, the binding energies ranged from 7.7-1.2 kJ/mol (645-96 cm^{-1}) for EQ0Ar-EQ7Ar. Therefore, IRPD of the Ar-tagged species is feasible because the absorption of an IR photon with 1200-3200 cm^{-1} is large enough to eliminate the Ar atom from the isomers. The calculated IR spectrum of EQ0Ar exhibited very strong HCH bending bands at 1200-1500 cm^{-1} (~2700 km/mol) along with CN stretching bands at 2200-2300 cm^{-1}. The IR spectra of chain oligomers EQ1Ar-EQ6Ar were very similar, with strong bands (~500 km/mol) at 2120 cm^{-1} due to CN stretching vibration, and weak bands at 1200-1500 and 2900-3100 cm^{-1}. In contrast, the IR spectrum of EQ7Ar exhibited strong CH stretching bands at 2900-3000 cm^{-1} that are comparable to CN stretching (2300 cm^{-1}) and CCH bending (1200-1400 cm^{-1}) bands. The vibrational frequencies and band intensities of the IR spectra of these isomers are attributable to the spatial distribution of the excess electron in the cluster anions (see Supporting Information). The similarity between the observed IRPD spectrum of $(AN)_3^-$Ar ions (Figure 2a) and the calculated IR spectra of chain oligomers EQ1Ar-EQ6Ar indicates that the $(AN)_3^-$Ar structures are those of the chain oligomers that are produced by the intracluster polymerization of cluster ion.

The absence of the Ar-tagged cyclic oligomers EQ7Ar in the IRPD spectrum of

(AN)$_3^-$Ar can be explained as follows.   To discuss this reason, intracluster reaction

mechanism of (AN)$_3^-$Ar should be considered.   In the intracluster reaction of Ar-tagged

(AN)$_3^-$ cluster ions, there are two competing reaction: (1) polymerization of (AN)$_3^-$ cluster

ions and (2) evaporation of Ar atoms from (AN)$_3^-$Ar$_m$ ($m \geq 1$) cluster ions.   At first, the

electron attachment to the neutral (AN)$_3$Ar$_m$ cluster (Ar-tagged EQN) occurs.   The

stabilization energy due to the electron attachment to neutral (AN)$_3$ (92.2 kJ/mol) is quite

large.   This stabilization energy was estimated from the energy difference between EQN

and EQ0.   Due to this large stabilization energy, it seems that almost all Ar atoms

evaporate from the Ar-tagged EQ0 ion.   However, the observation of (AN)$_3^-$Ar ions in the

mass spectrum indicates that few (AN)$_3^-$Ar ions (EQ0Ar) remain after the electron

attachment.   In these EQ0Ar ions, the intracluster polymerization occurs to produce the

EQ1Ar ions.   In the EQ0Ar $\rightarrow$ EQ1Ar reaction, the EQ1 is calculated to be unstable than

EQ0 (Figure 3).   Therefore, the Ar-evaporation does not occur in the EQ0Ar $\rightarrow$ EQ1Ar

reaction because the reaction is endothermic.   To form the EQ3Ar, 2-step reactions from

EQ1Ar should be occur.   These 2-step reactions (EQ1Ar $\rightarrow$ EQ2Ar $\rightarrow$ EQ3Ar) are also

endothermic (Figure 3).   For this reason, EQ3Ar is formed by the intracluster reaction in

(AN)$_3^-$Ar without the Ar-evaporation.   This is consistent with the observed IRPD

spectrum of (AN)$_3^-$Ar (Figure 2a) which can be assigned to chain oligomers (EQ1Ar,

EQ2Ar, EQ3Ar).   This trapping of high-energy isomers in Ar-tagged cluster ions due to

the low internal energy has been observed in recent studies.[26-28]   In the reaction of EQ3Ar

$\rightarrow$ EQ4Ar, the polymerization of EQ3Ar is found to be the exothermic reaction (Figure 3).

It seems that all EQ4 cluster ions are bare ions because large stabilization energy (80.0

kJ/mol) causes the evaporation of the Ar atom from EQ4Ar ions. Therefore, Ar-tagged cyclic oligomers cannot be formed due to the evaporation of the Ar atom in the EQ3Ar $\rightarrow$ EQ4Ar polymerization reaction.

For bare $(AN)_3^-$ ions, cyclization readily proceeds because the stabilization energy due to the electron attachment to neutral $(AN)_3$ (92.2 kJ/mol) is larger than all the barrier heights in the polymerization pathway. In the case of the "warm" $(AN)_3^-$, cyclization is unavoidable due to the small energy barriers in the polymerization pathway of $(AN)_3^-$. Unfortunately, the IR spectrum of bare $(AN)_3^-$ ions cannot be measured using the one-photon process. The IR multiphoton dissociation (IRMPD) method seems to be useful to measure the IR spectrum of bare $(AN)_3^-$ ions. Subsequently, it was questioned whether longer chain oligomers $(AN)_n^-$ ($n \geq 4$) cluster anions can be synthesized in the anionic polymerization. The mechanisms of branching between chain propagation and cyclization in intracluster anionic polymerization in $(AN)_n^-$ ions were considered. The barrier height of TS4/5 from EQ4 is the highest barrier in the polymerization pathway of $(AN)_3^-$ (Figure 3). From this reason, the rotational isomerization of EQ4 can be a bottleneck in the cyclization of $(AN)_3^-$. The polymerization pathway of $(AN)_3^-$ starting from EQ4 is shown in Figure 4a. Upon the formation of EQ5 by rotational isomerization of EQ4 via TS4/5, cyclic oligomer EQ7 was formed via a 2-step reaction, as shown in Figure 3. Therefore, to proceed the cyclization of $(AN)_3^-$, the rotational isomerization of EQ4 should occur before the cyclization. Because of the relatively small ring distortion, the formation of the 6-membered ring structure should be favorable. Similar intramolecular cyclization, known as Dieckmann condensation, have been observed in the

anionic polymerization of acrylates.[29]   As shown in Figure 4b, the proposed schematic

reaction pathways of intracluster polymerization of $(AN)_4^-$ feature three optimized $(AN)_4^-$

structures that were calculated at the M06-2X/6-31++G** level.   Isomer EQ4+AN,

which can be described as an AN-solvated EQ4 ion serves as the branching point between

the chain propagation and cyclization reaction pathways.   If the rotational isomerization

of EQ4 in EQ4+AN occurs faster than the addition of a fourth AN molecule to the EQ4,

cyclization of $(AN)_4^-$ will proceed and form isomer EQ7+AN.   On the other hand, if the

addition of a fourth AN molecule to EQ4 is faster than the rotational isomerization, the

$(AN)_4^-$ chain oligomer will be formed via chain propagation reaction.   Because the

SOMO of the $(AN)_4^-$ chain oligomer indicates that the distribution of the excess electrons

is found at the end of chain, the propagating chain oligomer should retain its active

carbanionic end group, and thus is a living oligomer.   The formation of a cyclic oligomer

for the $(AN)_4^-$ chain oligomer is somewhat unlikely because of the large distortion that

will be incurred by the 8-membered ring.[30]   Therefore, once an $(AN)_4^-$ chain oligomer is

formed in the initial stages of the anionic polymerization of the AN cluster anions, the

chain propagation reactions should proceed repeatedly via addition of additional AN

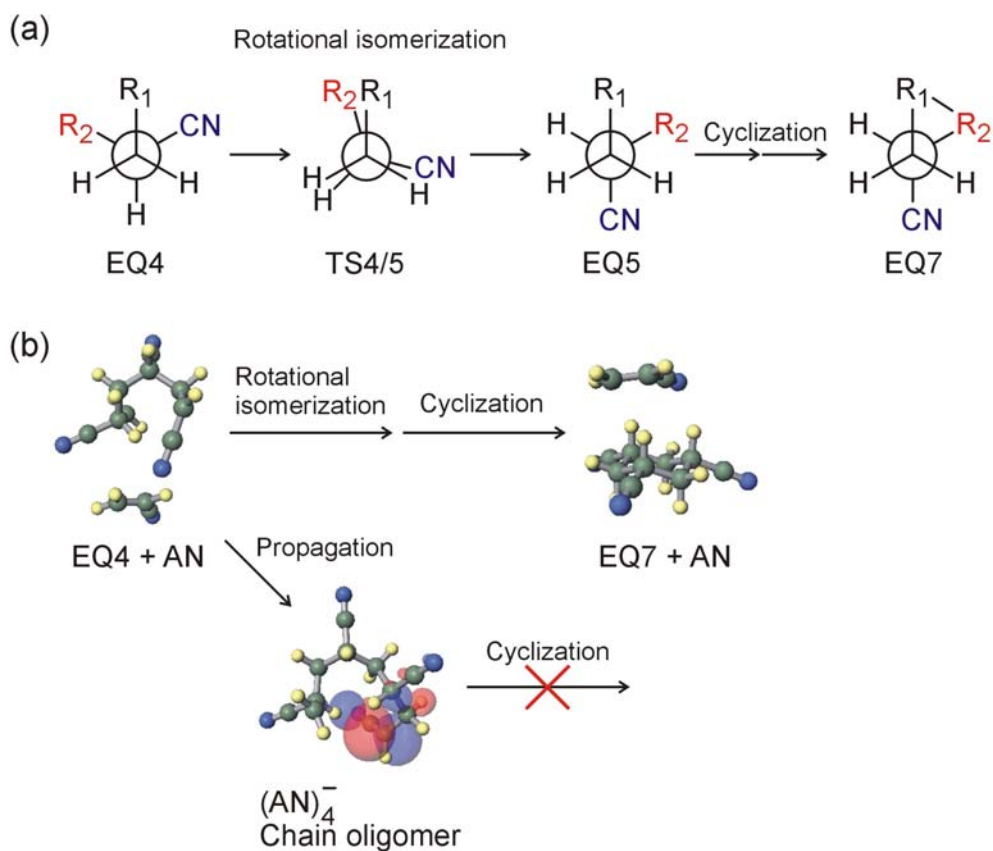monomers, and thus avoiding termination (cyclization reaction).

Figure 4. (a) Polymerization pathway of $(AN)_3^-$. Newman projections are shown for EQ4, TS4/5, EQ5, and EQ7; $R_1 = -CH(CN)-CH_2$, $R_2 = -CH_2-CH(CN)$. (b) Proposed branching mechanism in the intracluster anionic polymerization of $(AN)_4^-$. Structures were calculated using geometry optimizations at the M06-2X/6-31++G** level. Singly occupied molecular orbital (SOMO) of the $(AN)_4^-$ chain oligomer is also shown.

4. CONCLUSIONS

We have shown the possible mechanism of the anionic polymerization of $(AN)_3^-$ by IRPD spectroscopy combined with calculations of the polymerization pathway. IRPD spectroscopy using the Ar-tagging method enabled us to observe the chain oligomers for

the first time – specifically the IRPD spectrum of $(AN)_3^-Ar$ exhibited only the chain oligomers. Based on the SCW method of calculating the polymerization pathway of $(AN)_3^-$, "warm" $(AN)_3^-$ ions readily undergoes cyclization, whereas "cold" $(AN)_3^-Ar$ ions, with a low internal energy, result in trapped chain oligomers in a well on the potential energy surface. We have found that the rotational isomerization of the chain oligomer should occur to form the $(AN)_3^-$ cyclic oligomer. For the anionic polymerization of $(AN)_4^-$ cluster anions, the formation of the chain oligomer via chain propagation requires that the addition of a neutral AN molecule to the $(AN)_3^-$ chain oligomer should occur *before* the rotational isomerization. The combination of experimental and theoretical results have allowed the elucidation of the key branching point between cyclization (termination) and chain propagation in anionic polymerization.

Supporting Information Calculated singly occupied molecular orbitals (SOMO) of EQ0-EQ7. Relationship between IR spectra (vibrational frequencies and band intensities)

and SOMOs. A full list of authors in Ref. 24. This material is available free of charge via the Internet at http://pubs.acs.org.

REFERENCES

(1) Shabtai, J.; Ney-Igner, E.; Pines, H. *J. Org. Chem.* **1975**, *40*, 1158-1162.

(2) El-Shall, M. S. *Acc. Chem. Res.* **2008**, *41*, 783-792.

(3) McDonald, R. N.; Chowdhury, A. K. *J. Am. Chem. Soc.* **1982**, *104*, 2675-2676.

(4) Tsukuda, T.; Kondow, T. *Chem. Phys. Lett.* **1992**, *197*, 438-442.

(5) Tsukuda, T.; Kondow, T. *J. Phys. Chem.* **1992**, *96*, 5671-5673.

(6) Tsukuda, T.; Terasaki, A.; Kondow, T.; Scarton, M. G.; Dessent, C.E.; Bishea, G. A.; Johnson, M. A. *Chem. Phys. Lett.* **1993**, *201*, 351-356.

(7) Tsukuda, T.; Kondow, T. *J. Am. Chem. Soc.* **1994**, *116*, 9555-9564.

(8) Ichihashi, M.; Tsukuda, T.; Nonose, S.; Kondow, T. *J. Phys. Chem.* **1995**, *99*, 17354-17358.

(9) Fukuda, Y.; Tsukuda, T.; Terasaki, A.; Kondow, T. *Chem. Phys. Lett.* **1995**, *242*, 121-125.

(10) Fukuda, Y.; Tsukuda, T.; Terasaki, A.; Kondow, T. *Chem. Phys. Lett.* **1996**, *260*, 423-427.

(11) Tsukuda, T.; Kondow, T.; Dessent, C. E. H.; Bailey, C. G.; Johnson, M. A.; Hendricks, J. H.; Lyapustina, S. A.; Bowen, K. H. *Chem. Phys. Lett.* **1997**, *269*, 17-21.

(12) Ichihashi, M.; Sadanaga, Y.; Kondow, T. *J. Phys. Chem. A* **1998**, *102*, 8287-8292.

(13) Ohshimo, K.; Misaizu, F.; Ohno, K. *J. Phys. Chem. A* **2000**, *104*, 765-770.

(14) Tsunoyama, H.; Ohshimo, K.; Misaizu, F.; Ohno, K. *J. Am. Chem. Soc.* **2001**, *123*, 683-690.

(15) Fukuda, Y.; Ichihashi, M.; Terasaki, A.; Kondow, T.; Osoda, K.; Narasaka, K. *J. Phys.*

Chem. A **2001**, *105*, 7180-7184.

(16) Ohno, K.; Maeda, S. *Chem. Phys. Lett.* **2004**, *384*, 277-282.

(17) Maeda, S.; Ohno, K. *J. Phys. Chem. A* **2005**, *109*, 5742-5753.

(18) Ohno, K.; Maeda, S. *J. Phys. Chem. A* **2006**, *110*, 8933-8941.

(19) Maeda, S.; Ohno, K. *J. Chem. Phys.* **2006**, *124*, 174306.

(20) Kobayashi, Y.; Inokuchi, Y.; Ebata, T. *J. Chem. Phys.* **2008**, *128*, 164319.

(21) Hammer, N. I.; Shin, J. −W.; Headrick, J. M.; Diken, E. G.; Roscioli, J. R.; Weddle, G. H.; Johnson, M. A. *Science* **2004**, *306*, 675-679.

(22) Lisy, J. M. *J. Chem. Phys.* **2006**, *125*, 132302.

(23) Maeda, S.; Ohno, K. *Chem. Phys. Lett.* **2005**, *404*, 95-99.

(24) Frisch, M. J. et al. *Gaussian 09*, Revision B.01; Gaussian, Inc.: Wallingford CT, 2010.

(25) Khlifi, M.; Nollet, M.; Paillous, P.; Bruston, P.; Raulin, F.; Bénilan, Y.; Khanna, R. K. *J. Mol. Spectro.* **1999**, *194*, 206-210.

(26) Rodriguez, J. D.; Lisy, J. M. *Int. J. Mass Spectrom.* **2009**, *283*, 135-139.

(27) Rodriguez, O., Jr.; Lisy, J. M. *J. Phys. Chem. Lett.* **2011**, *2*, 1444-1448.

(28) Rodriguez, J. D.; Lisy, J. M. *J. Am. Chem. Soc.* **2011**, *133*, 11136-11146.

(29) Vollhardt, K. P. C.; Schore, N. E. *Organic Chemistry*; second edition; W. H. Freeman and Company: New York, 1994, p 916.

(30) Young, R. J.; Lovell, P. A. *Introduction to Polymers*; third edition; CRC Press: Boca Raton, FL, 2011, p 39.

Table of Contents Graphic